Development, Degeneration and Regeneration, and Aging

Moderate repulsive effects of E-unit–containing chondroitin sulfate (CSE) on behavior of retinal growth cones

Miki Shimbo[a], Satoru Ando[a], Nobuo Sugiura[b], Koji Kimata[b],Hiroyuki Ichijo[a, c] *

[a]Department of Anatomy and Embryology, Division of Biomedical Science, Faculty of Medicine, University of Tsukuba, Tsukuba, Ibaraki 305-8575, Japan

[b]Institute for Molecular Science of Medicine and Research Complex for the Medicine Frontiers, Aichi Medical University, Yazako, Nagakute, Aichi 480-1195, Japan

*Corresponding author: Hiroyuki Ichijo

[c]Present address of corresponding author: Hiroyuki Ichijo, Department of Anatomy, Graduate School of Medicine and Pharmaceutical Sciences, University of Toyama, Toyama 930-0194

E-mail address: ichijo@med.u-toyama.ac.jp

Tel: +81-76-434-7205, Fax: +81-76-434-5010

Running title: Diversity of chondroitin sulfate and growth cone behavior

Number of pages: 28

Number of figures: 6

Number of tables: 1

Number of words: Abstract (210), Introduction (775), Results (1247), Discussion (1074)

Abbreviations

A-unit of CS, GlcAβ1-3GalNAc(4-O-sulfate); C-unit of CS, GlcAβ1-3GalNAc(6-O-sulfate); BSA, bovine serum albumin; CS, chondroitin sulfate; CS-PE, lipid-derivatized chondroitin sulfate; CS-PE beads, polystyrene beads coated with lipid-derivatized chondroitin sulfate; CSPG, chondroitin sulfate proteoglycan; D-unit of CS, GlcA(2-O-sulfate)β1-3GalNAc(6-O-sulfate); E-unit of CS, GlcAβ1-3GalNAc(4,6-O-disulfate); GalNAc, *N*-acetylgalactosamine; GlcA, glucuronic acid; PBS, phosphate-buffered saline; PE, phosphatidylethanolamine; PTP, protein tyrosine phosphatase

Abstract

Chondroitin sulfate (CS), the carbohydrate chain of chondroitin sulfate proteoglycans, is involved in neuronal circuit formation during development. CS shows great structural diversity with combination of disaccharide units of different structure (A-, C-, D-, or E-unit). However, whether its structural diversity contributes to pathway formation remains unclear. We chemically coupled the reducing end of various types of CS to the amino group of phosphatidylethanolamine (lipid-derivatized CS, CS-PE) and established an in vitro time-lapse assay to observe the behaviors of growth cones of retinal ganglion cells from embryonic day 6 chick retina on exposure to beads coated with lipid-derivatized CS (CS-PE beads). Among CS-PEs with different content of the structural units, the beads coated with E-unit–containing CS-PE [E-unit: GlcAβ1-3GalNAc(4,6-O-disulfate)] (CSE-PE beads) significantly caused the growth cones to retract and to turn away from the beads, but the beads coated with CSA-, CSC- or CSD-PE beads did not. Importantly, not all the growth cones retracted equally from the CSE-PE beads, but they showed continuum of the repulsive behaviors; some behaved moderately and others remarkably. The growth cones distinguished different samples of CS: CSE and the others. Moreover, the continuum of the repulsive behaviors suggests that CS might be involved with the fine regulation of growth cones' behavior through its characteristic structure.

Keywords: proteoglycan, chondroitin sulfate, retina, axon, growth cone, circuit formation

Moderate repulsive effects of E-unit-containing chondroitin sulfate

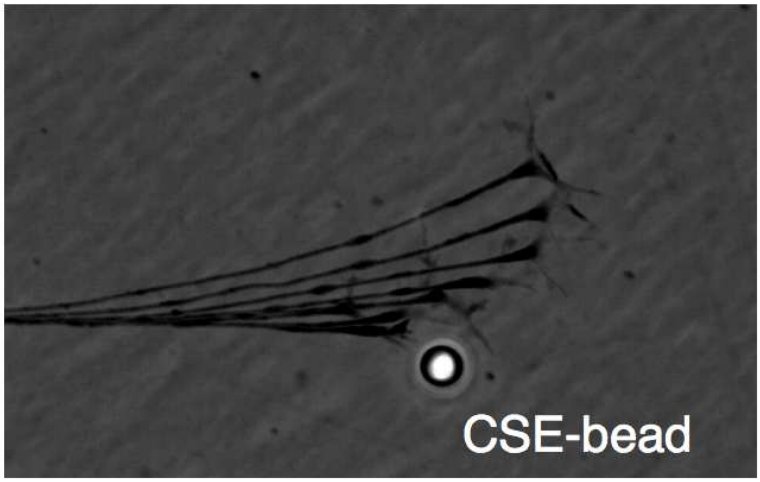

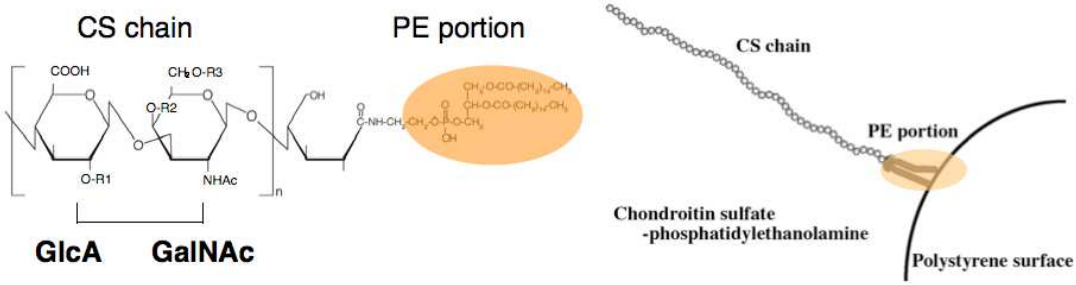

1. Introduction

Neurons extend their axons along a precise pathway with the help of guidance cues and receptors during development. Chondroitin sulfate proteoglycans (CSPGs) act as guidance cues or modulators that inhibit axonal growth at various decision points along the neuronal pathway (Ichijo, 2004; Holt and Dickson, 2005; Carulli et al., 2005). CSPG comprises a core protein and carbohydrate chains of CS. CS is an unbranched polymer comprising repeating disaccharide units of glucuronic acid (GlcA) and N-acetylgalactosamine (GalNAc).

The inhibitory effects of CS have been shown in the axonal outgrowth of retinal ganglion cells in vitro, pathway formation of retinal axons in vivo, glial roof plate, and axonal pathways in the spinal cord (Snow et al., 1990; Snow et al., 1991; Brittis et al., 1992; Brittis et al., 1994; Hoffman-Kim et al., 1998; Chung et al., 2000; Yick et al., 2000; Ichijo and Kawabata, 2001; Moon et al., 2001; Becker and Becker, 2002; Walz et al., 2002; Masuda et al., 2004). Because the inhibitory effect of CS is an important factor that prevents spinal axons from regenerating in the central nervous system after injury, researches have focused on the therapeutic utility of CS removal from glial scars (Bradbury et al., 2002; Morgenstern et al., 2002; Busch and Silver, 2007; Cafferty et al., 2008). Further, CS exhibits various effects on different neurons. CS promotes neurite outgrowth in vitro (Faissner et al., 1994; Fernaud-Espinosa et al., 1994; Challacombe and Elam, 1997; Clement et al., 1998; Nadanaka et al., 1998; Clement et al. 1999) and functions as a target-derived neurotrophic factor for retinal ganglion cells in rat (Huxlin et al., 1993). Effects of CS on circuit plasticity in the visual cortex have also been studied (Lander et al., 1997; Pizzorusso et al., 2002; Pizzorusso et al., 2006; Carulli et al., 2010).

It is well known that CS exhibits structural diversity. The disaccharide unit of CS (GlcA-GalNAc) is modified by sulfation at different positions, resulting in different structures of the units classified as O-unit (GlcA-GalNAc), A-unit (GlcA-GalNAc4S), C-unit (GlcA-GalNAc6S), D-unit (GlcA2S-GalNAc6S), and E-unit (GlcA-GalNAc4S6S) (Fig. 1). These

units combine, resulting in structural diversity. Structurally diverse CSs have different effects during neurite elongation (Wang et al., 2008; Lin et al., 2011) and cortical layer formation (Ishii and Maeda, 2008; Nishimura et al., 2010). E-unit containing CS promotes neurite outgrowth of hippocampal neurons in vitro (Clement et al. 1999), suggesting the differential effects between neuronal cell types. However, it remains unknown how the different structures of CSs exert diverse effects on different neuronal cells in different contexts through specific cellular responses. Recent findings suggest that cells might recognize the specific structure of CS (Clement et al., 1998; Nadanaka et al., 1998; Oohira et al., 2000; Ueoka et al., 2000; Gilbert et al., 2005; Properzi et al., 2005). Proteins binding to CS specifically recognize octa- or decasaccharides of CS chains with particular sequences but not non-specific characters such as their full lengths or net charges (Blanchard et al., 2007; Deepa et al., 2007a; Deepa et al., 2007b; Pothacharoen et al., 2007; Numakura et al., 2010). Thus, it is proposed that cells recognize CS through cell surface receptors such as transmembrane protein tyrosine phosphatase (PTP σ) and contactin-1, which have been shown to be involved in the receiving of the effects of CS (Mikami et al., 2009; Shen et al., 2009; Coles et al., 2011).

Among the many neuronal circuits, the retinotectal pathway is most amenable to experimental approaches. In the chick optic tract, axons of retinal ganglion cells are demarcated by CS labeled with MO-225 anti-CS monoclonal antibody; MO-225 epitopes are distributed on the diencephalotelencephalic boundary and in the neuropils encircling the optic tract (Ichijo, 2006). This observation suggests that the structural diversity of CS plays a role in CSPG-mediated ax-on guidance; however, the effect of CS structural diversity on retinal growth cones has not been investigated in detail. In this study, we chemically coupled the reducing end of various types of CS to the amino group of phosphatidylethanolamine (lipid-derivatized CS, CS-PE) (Sugiura et al., 1993; Oohira et al., 2000) and immobilized the CS-PE hydrophobically on polystyrene beads. We established an in vitro time-lapse assay to

observe the chick retinal growth cones that en-countered the CS-PE beads and examined the effects of CS structural diversity on growth cone behavior. The retinal growth cones moved away selectively from the CSE-PE beads, indicating that the growth cones distinguish CSE from the others and differentiate their structure. Importantly, not all the growth cones retracted equally from the CSE-PE beads, but they showed continuum of the repulsive behaviors, which suggests that CS might be involved with the fine regulation of growth cones' behavior through its characteristic structure.

2. Results

2.1. Structural diversity of CS examined using beads coated with lipid-derivatized CS

Four kinds of CS-PE beads were prepared: CSA-, CSC-, CSD-, and CSE-PE beads. Immunoreactivity of the CS-PE beads was examined using various anti-CS monoclonal antibodies of different specificities. To demonstrate the configuration of CS-PE and polystyrene beads, CSD-PE beads were treated with enzymes, followed by CS-56 immunostaining and flow cytometry (Fig. 2B). The signal intensity of CSD-PE beads disappeared completely after phospholipase D treatment. Because phospholipase D cleaves phosphatidylethanolamine and releases the CS portion from the beads, the result shows that the PE portion of the CS-PE molecules is immobilized on the beads by hydrophobic interaction. Furthermore, treatment with chondroitinase ABC caused variable reductions in CS immunoreactivity, seen as a broader peak (Fig. 2B), which indicates that CS carbohydrate chains are situated outside the PE portion and envelop the beads.

The beads coated with CSA-PE, CSC-PE, CSD-PE, and CSE-PE were differentially recognized using the following anti-CS antibodies: MO-225, CS-56, and 2H6 (Fig. 2C). The MO-225 anti-CS antibody preferentially binds to the C-, D-, and E-units of CS; the signals with MO-225 were intense on the CSC-PE, CSD-PE, and CSE-PE beads but only weak on the CSA-PE beads. The MO-225 anti-CS monoclonal antibody was originally reported to bind to D-unit-rich CS (Yamagata et al., 1987). It was later reported that MO225 recognizes group of

6 - 10 saccharides, sequences of the units like C-A-D-C, A-D-C, A-D-A, and E-E-E-E-C (Ito et al., 2005; Deepa et al., 2007ab). Thus, MO-225 is likely to recognize groups of the units including the E-unit but do not exclusively E-unit proper (Fig 2C).

The CS-56 anti-CS antibody preferentially binds to the C- and D-units; the signals with CS-56 were intense on the CSC-PE and CSD-PE beads but weak on the CSA-PE and CSE-PE beads (Fig 2C). The 2H6 anti-CS antibody preferentially binds to the A-units; the signals with 2H6 were intense on the CSA-PE beads but weak on the CSC-PE, CSD-PE, and CSE-PE beads (Fig 2C). These binding preferences confirmed the specificity of anti-CS antibodies. These results showed that the different structural diversity of CSA-PE, CSC-PE, CSD-PE, and CSE-PE was represented on the beads, which confirms that retinal growth cones were exposed to particular structures of CS when they encountered each bead.

2.2. Differential behaviors of retinal growth cones toward beads coated with lipid-derivatized CS

On the culture substrate, most of the beads stood still and some moved unsteadily. To exclude non-specific influences of the unsteady beads, for example, a mechanical impact, we examined only the beads standing still in the analyses. Retinal growth cones showed diverse behaviors when they encountered the beads but did not show stereotypical behavior against specific beads. The behaviors were approximately classified into 3 types: retraction, turn, and no change (Figs. 3, and supplemental movies). Since random nature of the growth cone responses was concerned, we firstly examined correlation between growth cones' behaviors and touching angles of growth cones to a bead coated with crude CS-PE. "Turn" reflected approximate turning angle more than 15° as shown in the experimental procedures. In the scatter plot (Fig. 2D), no correlation was observed between the touching angles and behaviors; thus, different trajectories of growth cone migration relative to a bead were not thought to result in the three types of behaviors.

Retinal growth cones encountering CSE-PE beads showed higher percentages of retraction (CSE-PE beads: 9.7%, n = 93) (Figs. 4A). Those encountering CSC-PE or CSD-PE beads showed moderate percentages of retraction (CSC-PE beads: 6.6%, n = 76; CSD-PE beads: 5.1%, n = 78), and those encountering raw beads or CSA-PE beads showed lower percentages of retraction (raw beads: 2.4%, n = 85; CSA-PE beads: 0%, n = 83). Treatment with chondroitinase ABC quenched the effect of CSE-PE beads on retraction (CSE-PE beads treated with chondroitinase ABC: 2.2%, n = 93). The percentage of growth cones' retraction was significantly greater with CSE-PE beads than with raw beads (by chi-square test, $p < 0.05$), CSA-PE beads ($p < 0.01$) and CSE-PE beads treated with chondroitinase ABC ($p < 0.05$). The percentage of retraction induced by CSC-PE or CSD-PE beads was not significantly different from that induced by raw beads.

Moreover, the growth cones retracted significantly more slowly on CSE-PE beads than the other beads (mean ± standard deviation: CSE-PE, 35.3 ± 17.8 min, n = 9) (non CSE-PE, 9.8 ± 5.9 min, n = 13) (Mann-Whitney U test, $p < 0.01$) (Supplemental movies and Figs. 4B). This was also the case except for the retraction. We determined how long the growth cone halted after contacting the bead. In the scatter plots, a fraction of the growth cones halted for longer on encountering CSE-PE beads than the others, although individual growth cones halted for various periods (Fig. 5A). The mean halt time of the growth cones was significantly longer on the CSE-PE beads than the others (CSE-PE bead: 10.9 ± 11.0 min, raw bead: 8.7 ± 4.1 min, CSA-PE bead: 7.7 ± 4.9 min, CSC-PE bead: 9.7 ± 5.2 min, CSD-PE bead: 8.6 ± 5.5 min) and the CSE-PE beads treated with chondroitinase ABC (9.1 ± 4.9 min) [ANOVA followed by Bonferroni's multiple comparison test: the CSE-PE bead against raw beads ($p < 0.05$), CSA-PE beads ($p < 0.01$), and CSD-PE bead ($p < 0.05$)] (Fig. 5B).

Except for retraction and halt, the growth cones altered their growth direction on encountering the beads, although some passed by the beads without changing their direction. In particular, growth cones encountering the CSE-PE beads turned away from the beads with a

large angle (Fig. 3C). To elucidate growth cone turning, the angles of growth direction change were measured and plotted (Fig. 5C). An angle above zero indicates that the growth cones moved away from the beads, and an angle below zero indicates that they moved toward the beads. Growth cones turned significantly away from CSE-PE beads (12.4° ± 19.9°). Small angles of deflection were observed for raw beads (1.1° ± 9.9°) and beads coated with CSA-PE (1.8° ± 12.1°), CSC-PE (4.0° ± 15.9°) or CSD-PE (3.0° ± 11.6°). The effect of CSE-PE beads on the turning angle was quenched by treatment with chondroitinase ABC (2.7° ± 11.9°). The turning angles for CSE-PE beads were significantly different from those for all other types of beads (ANOVA followed by Bonferroni's multiple comparison test, $p < 0.01$) (Fig. 5D).

Since the growth cones turning angles against CSE-PE bead seemed to be distributed in a bimodal manner at 20° (Fig. 5C) and the turning angle more than 20° were easily recognized in time-lapse movie at a glance, behaviors of growth cones were categorized into 3 types as retraction (A), turning away by more than 20° (B) and turning by less than 20° (C). The percentages shown (A+B)/(A+B+C) as "growth cones moving away remarkably" were evaluated using the chi-square test (Fig. 6). Retinal growth cones encountering CSE-PE beads showed higher percentage of the remarkable response (CSE-PE beads: 41.9%, $n = 93$). Those encountering CSC-PE beads showed moderate percentage (CSC-PE beads: 15.8%, $n = 76$), and those encountering raw beads, CSA-PE beads, or CS-D beads showed lower percentages (raw beads: 5.9%, $n = 85$; CSA-PE beads: 6.0%, $n = 83$; CSDE-PE beads: 9.0%, $n = 78$). Treatment with chondroitinase ABC quenched the effect of CSE-PE beads (CSE-PE beads treated with chondroitinase ABC: 10.8%, $n = 93$). The percentage of growth cones with the remarkable behaviors was significantly greater on the CSE-PE bead than on the others (by chi-square test, $p < 0.0001$).

3. Discussion

Four kinds of CS-PE beads were prepared: CSA-, CSC-, CSD-, and CSE-PE beads. Axonal growth cones probe CS-PE beads, which enables us to question whether growth cones sense and behave differently according to the structural diversity of CS. Thus, CS-PE beads are a feasible substrate for investigating the structural diversity of CS and its function. The present method allows us to specify when and where the CS affects individual growth cones in the time-lapse movies, which further opens the possibility to investigate the intracellular mechanism with high spatiotemporal resolution. Coating the CS-PE beads with BSA inhibited non-specific binding (data not shown); however, it is theoretically possible that unknown factors conditioned by retinal cells may bind only to specific types of CS and exert their influences on growth cone behavior as suggested in previous investigations (Ishii and Maeda, 2008; Wang et al., 2008; Mikami et al., 2009; Nishimura et al., 2010; Lin et al., 2011).

The inhibitory effects of CS have been shown on the axonal outgrowth of retinal ganglion cells in vitro (Ichijo and Kawabata, 2001; Lam et al., 2008) and pathway formation of retinal axons in vivo (Chung et al., 2000; Ichijo and Kawabata, 2001; Walz et al., 2002), indicating that CS delimits the border of the axonal pathway and prevents the axons from entering aberrant territory. Especially, CS recognized by MO-225 has been a structural candidate because its epitopes are distributed on the diencephalotelencephalic boundary, in the neuropil encircling the optic tract (Ichijo, 2006), and in the telencephalon (Ichijo, 2007). Here, we showed that CSE-PE beads recognized by MO-225 caused repulsion during retinal growth cone steering. The CSE-PE beads halted the growth cones for a longer period and induced the growth cone's retraction more frequently than the others (Figs. 3, 4, and 5). The CSE-PE beads caused the growth cones to turn away from the beads (Fig. 5). The CSE-PE beads induced significantly higher percentages of the remarkable repulsive behaviors (the retracted growth cones or growth cones turning angle more than 20°) than the others (Fig. 6). The results suggest that E-unit-containing CS might prevents retinal axons from invading aberrant territory and delimits the border of retinal trajectory by encircling the optic tract.

However, the effects of CSE-PE beads seem to differ from those of the well-known proteinaceous repulsive cues: semaphorins and ephrins (Fournier et al., 2000; Weinl et al., 2003). CSE-PE beads did not induce drastic effects on all axons but rather moderately regulated axonal behavior. Importantly, not all the growth cones equally retracted from, halted on, or turned from the CSE-PE beads, but they showed continuum of the repulsive behaviors (Fig. 5A and C); some behaved moderately and others remarkably. It is unknown how retinal growth cones behave differentially toward CSE-PE beads; however, there are two possibilities. The first is that retinal growth cones discriminate heterogeneity within the CSE chain on the beads. In flow cytometric analysis, CSE-PE beads showed broad peaks of immunoreactivity against CS-56 and 2H6, despite its sharp peak against MO-225 (Fig 2C). The broad peaks of immunoreactivity result from the heterogeneity within the CSE chains. In CSE chains with higher percentages of E-units, other units were combined and aligned (Table 1), which is responsible for the heterogeneity within the CSE; for example, differences in the sequence or clustering of disaccharide units. It is conceivable that the structural heterogeneity within the CS chain is biologically relevant to the fine regulation of CS function, because each CS was prepared from biological samples. The second possibility is that retinal growth cones vary their sensitivity to E-unit-containing CS. Neurite outgrowth of hippocampal neurons is promoted on E-unit containing CS in vitro (Clement et al. 1999), suggesting that differential effects between neuronal cell types. Transmembrane protein tyrosine phosphatase (PTPσ) and contactin-1 were shown to be the functional receptors of CSPG and CSE, respectively (Mikami et al., 2009; Shen et al., 2009; Coles et al., 2011); it would be intriguing if this is the case in pathway formation of retinal axons. It has been reported in vitro, using CS-biotin-streptavidin complex, that some retinal axons growing on CS-containing substrate reduce the MO-225 staining along axons (Ando 2010), which is thought to be an adaptation for the retinal axons to alter their microenvironment for growth. Alteration of the CS microenvironment may reduce sensitivity to CSE-PE beads and lead to diverse behaviors.

In vivo, the chronological order of retinal axon growth is well studied in the optic tract. The late-growing retinal axons run through the superficial layer of the optic tract, whereas the early-growing axons run through the deep layer of the optic tract in contact with MO-225-positive neuropil (Rager, 1980; Leung et al., 2003; Ichijo, 2006), which suggests that the axons in the deep layer run on the neuropil with MO-225-positive CS. The differential repulsive effect of CS containing E-units might be involved with the chronological sorting. Role of CS in activity-dependent fine-tuning have also been shown in ocular dominance plasticity in the visual cortex (Pizzorusso et al., 2002; Pizzorusso et al., 2006; Carulli et al., 2010); it would be intriguing to determine whether the structural diversity of CS is involved in this process, as well.

It is important but difficult to investigate relationship between structural diversity of CS and its functional specificity. Here we showed the effects of biological sample of E-unit-containing CS (CSE from squid). We used commercially available samples of CS; thus, mean molecular weights of CS-PEs were not exactly the same (Table 1). Since recent findings suggest that cells might recognize a specific structure of CS (Blanchard et l., 2007; Clement et al., 1998; Deepa et al., 2007a; Deepa et al., 2007b; Nadanaka et al., 1998; Numakura et al., 2010; Oohira et al., 2000; Ueoka et al., 2000; Gilbert et al., 2005; Properzi et al., 2005; Pothacharoen et al., 2007), different lengths of CS chain are not thought to result in their effects; however, to use better preparations of CS with similar lengths would be considered in further investigations.

There is no assurance that the same structure in the CSE used in the experiments exists and functions in vivo, but the results indicate that the growth cones differentiate CS with various unit contents, suggesting that the growth cones might sense different structure of CS. It must be further investigated how detailed structure of CS is and how its structure is involved with regulation of the growth cones' behaviors. Synthesized CS oligosaccharides with defined sequences would be ideal for this purpose.

4. Experimental Procedure

4.1. Formation of polystyrene beads coated with lipid-derivatized CS

CS preparations: CS, CSA, CSC, CSD, and CSE were purchased from Seikagaku (Tokyo, Japan). The disaccharide unit composition of each CS was analyzed with fluorometric post-column high-performance liquid chromatography (Table 1). Since we used commercially available samples of CS and their coupling efficiency to PE was low, mean molecular weights of CS-PEs were not exactly the same. Partial digestion of CS chains was not performed because recent findings showed that cells or binding proteins recognize the structural motifs of octa- or decasaccharides but do not recognize whole length of CS chain. We did the experiments based on these facts. The reducing ends of CS were chemically coupled to the amino group of phosphatidylethanolamine (PE) to obtain lipid-derivatized CS (CS-PE) (Fig. 2A) (Sugiura et al., 1993). Polystyrene beads (5–6 μm in diameter; Spherotech Inc., Lake Forest, IL) were incubated overnight at 37.5 °C in CS-PE solution (200 μg/ml CS-PE in PBS). Once the beads were coated with CS-PE (CS-PE beads), they were treated with bovine serum albumin (BSA) to block nonspecific binding.

Immunoreactivity of the CS-PE beads was examined using anti-CS monoclonal antibodies of different specificities. CS-PE beads were washed in PBS and treated with 3.7% formaldehyde in PBS at room temperature for 2 h. They were washed twice in PBS, treated with 10% normal goat serum (Invitrogen, Carlsbad, CA) and incubated with anti-CS monoclonal antibody. Monoclonal antibodies against CS (2H6, MC21C, and MO-225) (Yamagata et al., 1987; Mark et al., 1989; Maeda et al., 1992; Oohira et al., 1994) were purchased from Seikagaku. CS-56 monoclonal antibody (Avnur and Geiger, 1984) was purchased from Sigma (St. Louis, MO). After the treatment with anti-CS antibodies, CS-PE beads were washed 3 times in PBS. Subsequently, they were incubated with goat anti-mouse IgG antibody conjugated with Alexa Fluor 488 (Invitrogen) as the secondary antibody. At some instances, before immunostaining, the CS-PE beads were treated overnight at 37 °C with phospholipase D (25 U, BIOMOL International, Plymouth Meeting, PA) or chondroitinase ABC (50 mU, Seikagaku) with

gentle agitation. The immunostained CS-PE beads were analyzed using a flow cytometer (Becton Dickinson, Franklin Lakes, NJ) and relevant software (FlowJo, Ashland, OR).

4.2. Retinal explant culture and time-lapse recording

Fertilized chicken eggs were obtained from a local farm. They were incubated at 37 °C. Retinal explants were prepared from embryonic day 6 chicks as described previously (Ichijo and Kawabata, 2001) and cultured at 37.5 °C on a substrate coated with poly-D-lysine (10 µg/ml, Sigma) and laminin (40 µg/ml, Invitrogen) in a serum-free chemically defined medium: 25 mM HEPES (4-[2-hydroxyethyl]-1-piperazineethanesulfonic acid)-buffered F12 nutrient mixture with N2 supplement (Invitrogen). The CS-PE beads were scattered on the culture substrate around the explant at a density of 150–200 particles/cm^2. A phase contrast inverted microscope (TE-2000E, Nikon, Tokyo, Japan) was used to observe the retinal axon growth cones, which grew out of the explant and encountered the beads. The time-lapse images of retinal growth cones were recorded using a digital camera and its controlling software (D50 and NIS-Elements, Nikon). To quantify growth cone retraction, the percentages of retracted growth cones and mean halt time of the retraction were evaluated using the chi-square test and Mann-Whitney *U* test, respectively. Halt time of the growth cone after encountering the beads was determined using a series of time-lapse images. Angles of axon direction change were measured using ImageJ (Wayne Rasband, NIH) before and after the growth cone encountered the beads. An angle above zero indicates that the growth cones moved away from the beads, and an angle below zero indicates that they moved toward the beads. The data were evaluated using ANOVA, followed by Bonferroni's test.

Since the growth cones turning angles against CSE-PE bead seemed to be distributed in a bimodal manner at 20° (Fig. 5C), behaviors of growth cones were categorized into 3 types as retraction (A), turning away by more than 20° (B) and turning by less than 20° (C). The per-

centages shown (A+B)/(A+B+C) as "growth cones moving away remarkably" were evaluated using the chi-square test.

All the experimental procedures were approved by the Committee for Animal Care and Use of the University of Tsukuba.

Acknowledgments

This work was supported by Grants-in-Aid for Scientific Research (C)(1850023) from the Japan Society for the Promotion of Science.

References

Ando, S., Sugiura, N., Kimata, K., Ichijo, H., 2010. Influences of retinal axons on the cultural substrate containing biotin-conjugated chondroitin sulfate in vitro. Anat. Sci. Int. 85, 189-193.

Avnur, Z., Geiger, B., 1984. Immunocytochemical localization of native chondroitin-sulfate in tissues and cultured cells using specific monoclonal antibody. Cell 38, 811-822.

Becker, C.G., Becker, T., 2002. Repellent guidance of regenerating optic axons by chondroitin sulfate glycosaminoglycans in zebrafish. J. Neurosci. 22, 842-853.

Blanchard, V., Chevalier, F., Imberty, A., Leeflang, B.R., Basappa, Sugahara, K., Kamerling, J.P., 2007. Conformational studies on five octasaccharides isolated from chondroitin sulfate using NMR spectroscopy and molecular modeling. Biochemistry 46, 1167-1175.

Bradbury, E.J., Moon, L.D., Popat, R.J., King, V.R., Bennett, G.S., Patel, P.N., Fawcett, J.W., McMahon, S.B., 2002. Chondroitinase ABC promotes functional recovery after spinal cord injury. Nature 416, 636-640.

Brittis, P.A., Canning, D.R., Silver, J., 1992. Chondroitin sulfate as a regulator of neuronal patterning in the retina. Science 255, 733-736.

Brittis, P.A., Silver, J., 1994. Exogenous glycosaminoglycans induce complete inversion of retinal ganglion cell bodies and their axons within the retinal neuroepithelium. Proc. Natl. Acad. Sci. USA 91, 7539-7542.

Busch, S.A., Silver, J., 2007. The role of extracellular matrix in CNS regeneration. Curr. Opin. Neurobiol. 17, 120-127.

Cafferty, W.B., Bradbury, E.J., Lidierth, M., Jones, M., Duffy, P.J., Pezet, S., McMahon, S.B., 2008. Chondroitinase ABC-mediated plasticity of spinal sensory function. J. Neurosci. 28, 11998-12009.

Carulli, D., Laabs, T., Geller, H.M., Fawcett, J.W., 2005. Chondroitin sulfate proteoglycans in neural development and regeneration. Curr. Opin. Neurobiol. 15, 116-120.

Carulli, D., Pizzorusso, T., Kwok, J.C., Putignano, E., Poli, A., Forostyak, S., Andrews, M.R., Deepa, S.S., Glant, T.T., Fawcett, J.W., 2010. Animals lacking link protein have attenuated perineuronal nets and persistent plasticity. Brain 133, 2331-2347.

Challacombe, J.F., Elam, J.S., 1997. Chondroitin 4-sulfate stimulates regeneration of goldfish retinal axons. Exp. Neurol. 143, 10-17.

Chung, K.Y., Taylor, J.S., Shum, D.K., Chan, S.O., 2000. Axon routing at the optic chiasm after enzymatic removal of chondroitin sulfate in mouse embryos. Development 127, 2673-2683.

Clement, A.M., Nadanaka, S., Masayama, K., Mandl, C., Sugahara, K., Faissner, A., 1998. The DSD-1 carbohydrate epitope depends on sulfation, correlates with chondroitin sulfate D motifs, and is sufficient to promote neurite outgrowth. J. Biol. Chem. 273, 28444-28453.

Clement, A.M., Sugahara, K., Faissner, A., 1999. Chondroitin sulfate E promotes neurite outgrowth of rat embryonic day 18 hippocampal neurons. Neurosci. Lett. 269, 125-128.

Coles, C.H., Shen, Y., Tenney, A.P., Siebold, C., Sutton, G.C., Lu, W., Gallagher, J.T., Jones, E.Y., Flanagan, J.G., Aricescu, A.R., 2011. Proteoglycan-specific molecular switch for RPTPs clustering and neuronal extension. Science 332, 484-488.

Deepa, S.S., Kalayanamitra, K., Ito, Y., Kongtawelert, P., Fukui, S., Yamada, S., Mikami, T., Sugahara, K., 2007a. Novel sulfated octa- and decasaccharides from squid cartilage chondroitin sulfate E: sequencing and application for determination of the epitope structure of the monoclonal antibody MO-225. Biochemistry 46, 2453-2465.

Deepa, S.S., Yamada, S., Fukui, S., Sugahara, K., 2007b. Structural determination of novel sulfated octasaccharides isolated from chondroitin sulfate of shark cartilage and their application for characterizing monoclonal antibody epitopes. Glycobiology 17, 631-645.

Faissner, A., Clement, A., Lochter, A., Streit, A., Mandl, C., Schachner, M., 1994. Isolation of a neural chondroitin sulfate proteoglycan with neurite outgrowth promoting properties. J. Cell Biol. 126, 783-799.

Fernaud-Espinosa, I., Nieto-Sampedro, M., Bovolenta, P., 1994. Differential effects of glycosaminoglycans on neurite outgrowth from hippocampal and thalamic neurones. J. Cell Sci. 107, 1437-1448.

Fournier, A.E., Nakamura, F., Kawamoto, S., Goshima, Y., Kalb, R.G., Strittmatter, S.M. 2000. Semaphorin3A enhances endocytosis at sites of receptor-F-actin colocalization during growth cone collapse. J. Cell Biol. 149, 411-422.

Gilbert, R.J., McKeon, R.J., Darr, A., Calabro, A., Hascall, V.C., Bellamkonda, R.V., 2005. CS-4,6 is differentially upregulated in glial scar and is a potent inhibitor of neurite extension. Mol. Cell. Neurosci. 29, 545-58.

Hoffman-Kim, D., Lander, A.D., Jhaveri, S., 1998. Patterns of chondroitin sulfate immunoreactivity in the developing tectum reflect regional differences in glycosaminoglycan biosynthesis. J. Neurosci. 18, 5881-5890.

Holt, C.E., Dickson, B.J., 2005. Sugar codes for axons? Neuron 46, 169-172.

Huxlin, K.R., Sefton, A.J., Schulz, M., Bennett, M.R., 1993. Effect of proteoglycan purified from rat superior colliculus on the survival of murine retinal ganglion cells. Brain Res. Dev. Brain Res. 74, 207-217.

Ichijo, H., 2004. Proteoglycans as cues for axonal guidance in formation of retinotectal or retinocollicular projections. Mol. Neurobiol. 30, 23-33.

Ichijo, H., 2006. Restricted distribution of D-unit–rich chondroitin sulfate carbohydrate chains in the neuropil encircling the optic tract and on a subset of retinal axons in chick embryos. J. Comp. Neurol. 495, 470-479.

Ichijo, H., 2007. Structural diversity of chondroitin sulfates and formation of retinotectal pathway. In: Maeda, N. (Eds), Neural Proteoglycans. Research Signpost, Kerala, pp. 139-152.

Ichijo, H., Kawabata, I., 2001. Roles of the telencephalic cells and their chondroitin sulfate proteoglycans in delimiting an anterior border of the retinal pathway. J. Neurosci. 21, 9304-9314.

Ishii, M., Maeda, N., 2008. Oversulfated chondroitin sulfate plays critical roles in the neuronal migration in the cerebral cortex. J. Biol. Chem. 283, 32610-32620.

Ito, Y., Hikino, M., Yajima, Y., Mikami, T., Sirko, S., von Holst, A., Faissner, A., Fukui, S., Sugahara, K., 2005. Structural characterization of the epitopes of the monoclonal antibodies 473HD, CS-56, and MO-225 specific for chondroitin sulfate D-type using the oligosaccharide library. Glycobiology 15, 593-603.

Lam, J.S., Wang, L., Lin, L., Chan, S.O., 2008. Role of protein kinase C in selective inhibition of mouse retinal neurites during contacts with chondroitin sulfates. Neurosci. Lett. 434, 150-154.

Lander, C., Kind, P., Maleski, M., Hockfield, S., 1997. A family of activity-dependent neuronal cell-surface chondroitin sulfate proteoglycans in cat visual cortex. J. Neurosci. 17, 1928-1939.

Leung, K.M., Taylor, J.S., Chan, S.O., 2003. Enzymatic removal of chondroitin sulphates abolishes the age-related axon order in the optic tract of mouse embryos. Eur. J. Neurosci. 17, 1755-1767.

Lin, R., Rosahl, T.W., Whiting, P.J., Fawcett, J.W., Kwok, J.C., 2011. 6-Sulphated chondroitins have a positive influence on axonal regeneration. PLoS One 6, e21499. doi:10.1371/journal.pone.0021499

Maeda, N., Matsui, F., Oohira, A., 1992. A chondroitin sulfate proteoglycan that is developmentally regulated in the cerebellar mossy fiber system. Dev. Biol. 151, 564-574.

Mark, M.P., Butler, W.T., Ruch, J.V., 1989. Transient expression of a chondroitin sulfate-related epitope during cartilage histomorphogenesis in the axial skeleton of fetal rats. Dev. Biol. 133, 475-488.

Masuda, T., Fukamauchi, F., Takeda, Y., Fujisawa, H., Watanabe, K., Okado, N., Shiga, T., 2004. Developmental regulation of notochord-derived repulsion for dorsal root ganglion axons. Mol. Cell. Neurosci. 25, 217-227.

Mikami, T., Yasunaga, D., Kitagawa, H., 2009. Contactin-1 is a functional receptor for neuroregulatory chondroitin sulfate-E. J. Biol. Chem. 284, 4494-4499.

Moon, L.D., Asher, R.A., Rhodes, K.E., Fawcett, J.W., 2001. Regeneration of CNS axons back to their target following treatment of adult rat brain with chondroitinase ABC. Nat. Neurosci. 4, 465-466.

Morgenstern, D.A., Asher, R.A., Fawcett, J.W., 2002. Chondroitin sulphate proteoglycans in the CNS injury response. Prog. Brain Res. 137, 313-332.

Nadanaka, S., Clement, A., Masayama, K., Faissner, A., Sugahara, K., 1998. Characteristic hexasaccharide sequences in octasaccharides derived from shark cartilage chondroitin sulfate D with a neurite outgrowth promoting activity. J. Biol. Chem. 273, 3296-3307.

Nishimura, K., Ishii, M., Kuraoka, M., Kamimura, K., Maeda, N., 2010. Opposing functions of chondroitin sulfate and heparan sulfate during early neuronal polarization. Neuroscience 169, 1535-1547.

Numakura, M., Kusakabe, N., Ishige, K., Ohtake-Niimi, S., Habuchi, H., Habuchi, O., 2010. Preparation of chondroitin sulfate libraries containing disulfated disaccharide units and inhibition of thrombin by these chondroitin sulfates. Glycoconj. J. 27, 479-489.

Oohira, A., Matsui, F., Watanabe, E., Kushima, Y., Maeda, N., 1994. Developmentally regulated expression of a brain specific species of chondroitin sulfate proteoglycan, neurocan, identified with a monoclonal antibody IG2 in the rat cerebrum. Neuroscience 60, 145-157.

Oohira, A., Kushima, Y., Tokita, Y., Sugiura, N., Sakurai, K., Suzuki, S., Kimata, K., 2000. Effects of lipid-derivatized glycosaminoglycans (GAGs) a novel probe for functional analyses of GAGs on cell-to-substratum adhesion and neurite elongation in primary cultures of fetal rat hippocampal neurons. Arch. Biochem. Biophys. 378, 78-83.

Pizzorusso, T., Medini, P., Berardi, N., Chierzi, S., Fawcett, J.W., Maffei, L., 2002. Reactivation of ocular dominance plasticity in the adult visual cortex. Science 298, 1248-1251.

Pizzorusso, T., Medini, P., Landi, S., Baldini, S., Berardi, N., Maffei, L., 2006. Structural and functional recovery from early monocular deprivation in adult rats. Proc. Natl. Acad. Sci. USA 103, 8517-8522.

Pothacharoen, P., Kalayanamitra, K., Deepa, S.S., Fukui, S., Hattori, T., Fukushima, N., Hardingham, T., Kongtawelert, P., Sugahara, K., 2007. Two related but distinct chondroitin sulfate mimetope octasaccharide sequences recognized by monoclonal antibody WF6. J. Biol. Chem. 282, 35232-35246.

Properzi, F., Carulli, D., Asher, R.A., Muir, E., Camargo, L.M., van Kuppevelt T.H., ten Dam G.B., Furukawa, Y., Mikami, T., Sugahara, K., Toida, T., Geller, H.M., Fawcett, J.W., 2005. Chondroitin 6-sulphate synthesis is up-regulated in injured CNS, induced by injury-related cytokines and enhanced in axon-growth inhibitory glia. Eur. J. Neurosci. 21, 378-390.

Rager, G., 1980. Retinotopy and order in the visual pathway of the chick embryo during development. Folia Morphol. (Praha) 28, 72-75.

Shen, Y., Tenney, A.P., Busch, S.A., Horn, K.P., Cuascut, F.X., Liu, K., He, Z., Silver, J., Flanagan, J.G., 2009. PTPs is a receptor for chondroitin sulfate proteoglycan, an inhibitor of neural regeneration. Science 326, 592-596.

Snow, D.M., Lemmon, V., Carrino, D.A., Caplan, A.I., Silver, J., 1990. Sulfated proteoglycans in astroglial barriers inhibit neurite outgrowth in vitro. Exp. Neurol. 109, 111-130.

Snow, D.M., Watanabe, M., Letourneau, P.C., Silver, J., 1991. A chondroitin sulfate proteoglycan may influence the direction of retinal ganglion cell outgrowth. Development 113, 1473-1485.

Sugiura, N., Sakurai, K., Hori, Y., Karasawa, K., Suzuki, S., Kimata, K., 1993. Preparation of lipid-derivatized glycosaminoglycans to probe a regulatory function of the carbohydrate moieties of proteoglycans in cell-matrix interaction. J. Biol. Chem. 268, 15779-15787.

Ueoka, C., Kaneda, N., Okazaki, I., Nadanaka, S., Muramatsu, T., Sugahara, K., 2000. Neuronal cell adhesion, mediated by the heparin-binding neuroregulatory factor midkine, is specifically inhibited by chondroitin sulfate E. J. Biol. Chem. 275, 37407-37413.

Walz, A., Anderson, R.B., Irie, A., Chien, C.B., Holt, C.E., 2002. Chondroitin sulfate disrupts axon pathfinding in the optic tract and alters growth cone dynamics. J. Neurobiol. 53, 330-342.

Wang, H., Katagiri, Y., McCann, T.E., Unsworth, E., Goldsmith, P., Yu, Z.X., Tan, F., Santiago, L., Mills, E.M., Wang, Y., Symes, A.J., Geller, H.M., 2008. Chondroitin-4-sulfation negatively regulates axonal guidance and growth. J. Cell Sci. 121, 3083-3091.

Weinl, C., Drescher, U., Lang, S., Bonhoeffer, F., Loschinger, J., 2003. On the turning of Xenopus retinal axons induced by ephrin-A5. Development 130, 1635-1643.

Yamagata, M., Kimata, K., Oike, Y., Tani, K., Maeda, N., Yoshida, K., Shimomura, Y., Yoneda, M., Suzuki, S., 1987. A monoclonal antibody that specifically recognizes a

glucuronic acid 2-sulfate-containing determinant in intact chondroitin sulfate chain. J. Biol. Chem. 262, 4146-4152.

Yick, L.W., Wu, W., So, K.F., Yip, H.K., Shum, D.K., 2000. Chondroitinase ABC promotes axonal regeneration of Clarke's neurons after spinal cord injury. Neuroreport 11, 1063-1067.

Figure legends

Figure 1

Schematic representation of CS units, structures, and related enzymes. CSs are unbranched polysaccharides composed of repeating units of disaccharide (glucuronic acid and N-acetylgalactosamine) that are classified into A-, C-, D-, and E-units depending on sulfation sites; structural diversity of CSs results from combinations of these units. A-unit of CS [GlcA β 1-3GalNAc(4-O-sulfate)] is synthesized by chondroitin 4-O-sulfotransferases. C-unit of CS [GlcA β 1-3GalNAc(6-O-sulfate)] is synthesized by chondroitin 6-O-sulfotransferases. D-unit of CS [GlcA(2-O-sulfate) β 1-3GalNAc(6-O-sulfate)] is synthesized by sequential modification with chondroitin 6-O-sulfotransferases and uronyl 2-O-sulfotransferase. E-unit of CS [GlcA β 1-3GalNAc(4,6-O-disulfate)] is synthesized by sequential modification with chondroitin 4-O-sulfotransferases and N-acetylgalactosamine 4-sulfate 6-O-sulfotransferase.

Figure 2

Beads coated with lipid-derivatized CS. The structural diversity of CS is demonstrated using fluorescence-activated sorter analysis with monoclonal anti-CS antibodies. (A) Schematic representation of lipid-derivatized CS consisting of a CS chain and a phosphatidylethanolamine (PE portion). Sulfation occurs on the R2 site in the A unit of CS (GlcA-GalNAc[4S]), R3 site in C unit (GlcA-GalNAc[6S]), R1 and R3 sites in D unit (GlcA[2S]-GalNAc[6S]), and R2 and R3 sites in E unit (GlcA-GalNAc[4S,6S]). The cleavage sites of chondroitinase ABC (asterisk) and phospholipase D (sharp) are indicated. (B) Immunoreactivity against anti-CS monoclonal antibody (CS-56) is shown for CSD-PE beads not treated with any enzyme (red), those treated with chondroitinase ABC (blue), and those treated with phospholipase D (green). (C) Immunoreactivity of anti-CS monoclonal

antibodies with different specificities (MO-225: left, CS-56: middle, 2H6: right) shows that different preparations of CS exhibit structural diversity (uncoated: light blue, CSA-PE: black, CSC-PE: dark blue, CSD-PE: green, CSE-PE: purple). (D) Scatter plot between growth cone's behaviors and contact angle of a growth cone to a CS-PE bead. Contact angles "zero" and "90°" indicate that "growth cone encountering in the front of the bead" and "growth cone touching the bead laterally at a right angle", respectively. Horizontal dotted lines indicate mean contact angles of growth cone to the beads. CS, chondroitin sulfate; CS-PE, lipid-derivatized chondroitin sulfate

Figure 3

Behaviors of retinal growth cones. Retraction of retinal growth cone encountering a CSE-PE bead (A) and turning of retinal growth cones encountering a CSC-PE bead (B), CSE-PE bead (C), and CSE-PE bead treated with chondroitinase ABC (D) are shown in a series of time-lapse images. Their turning angles are measured in superpositions of time-lapse images: 6.7° for the CSC-PE bead, 20.2° for the CSE-PE bead, and 2.6° for the CSE-PE bead treated with chondroitinase ABC. Scale bars, 6 μm.

CS, chondroitin sulfate; CS-PE, lipid-derivatized chondroitin sulfate

Figure 4

Retinal growth cones retract from CSE-PE beads. (A) Percentages of the retraction are shown on beads without any coating (-), beads coated with CSA-PE, CSC-PE, CSD-PE, CSE-PE, and CSE-PE treated with chondroitinase ABC. Asterisk (*) and double asterisk (**) indicate significant differences in the percentages of the retraction (chi-square test, *: $p < 0.05$ and **: $p < 0.01$). (B) The growth cones retract more slowly on CSE-PE beads than the other beads. CSE-PE beads halt the growth cones for a significantly longer period

during the retraction. Double asterisk (**) indicates significant difference between CSE-PE and the other beads in contact and halt during the retraction (Mann-Whitney *U* test, $p < 0.01$). CS, chondroitin sulfate; CS-PE, lipid-derivatized chondroitin sulfate

Figure 5

Retinal growth cones halt on and turn away from CSE-PE beads. (A) Halt time of retinal growth cones is plotted against beads without any coating (-), beads coated with CSA-PE, CSC-PE, CSD-PE, CSE-PE, and CSE-PE treated with chondroitinase ABC. (B) Mean halt time and their standard errors are shown. Asterisk (*) and double asterisk (**) indicate a significant difference in the halt of CSE-PE beads against (-) beads (*: $p < 0.05$), CSA-PE beads (**: $p < 0.01$), and CSD-PE beads (*: $p < 0.05$) (ANOVA followed by Bonferroni's test). (C) Turning angles of retinal growth cones are plotted against beads without any coating (-), beads coated with CSA-PE, CSC-PE, CSD-PE, CSE-PE, and CSE-PE treated with chondroitinase ABC. An angle above zero indicates that the growth cones turn away from the beads, and an angle below zero indicates that they turn toward the beads. (D) Mean turning angles and their standard errors are shown. Double asterisk (**) indicates significant differences between the turning angle of CSE-PE and those of other groups (ANOVA followed by Bonferroni's test, $p < 0.01$).
CS, chondroitin sulfate; CS-PE, lipid-derivatized chondroitin sulfate

Figure 6

Percentages of "the retracted growth cones" plus "growth cones of turning angle more than 20°" are evaluated. Triple asterisk (***) indicates significant differences between CSE-PE beads and the other beads (chi-square test, $p < 0.0001$).

unit	structure	related enzymes
A-	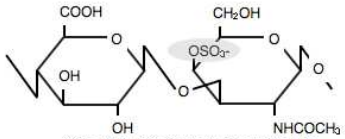 -4 GlcAβ1-3GalNAc(4-O-sulfate) β1-	chondroitin 4-O-sulfotransferases
C-	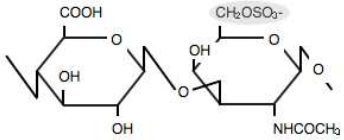 -4 GlcAβ1-3GalNAc(6-O-sulfate) β1-	chondroitin 6-O-sulfotransferases
D-	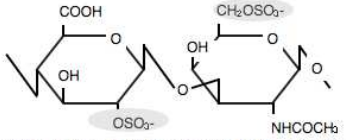 -4 GlcA(2-O-sulfate)β1-3GalNAc(6-O-sulfate) β1-	chondroitin 6-O-sulfotransferases uronyl 2-O-sulfotransferase
E-	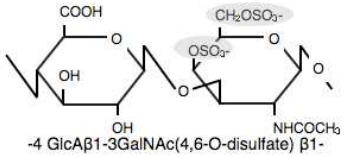 -4 GlcAβ1-3GalNAc(4,6-O-disulfate) β1-	chondroitin 4-O-sulfotransferases N-acetylgalactosamine 4-sulfate 6-O-sulfotransferase

Figure 1

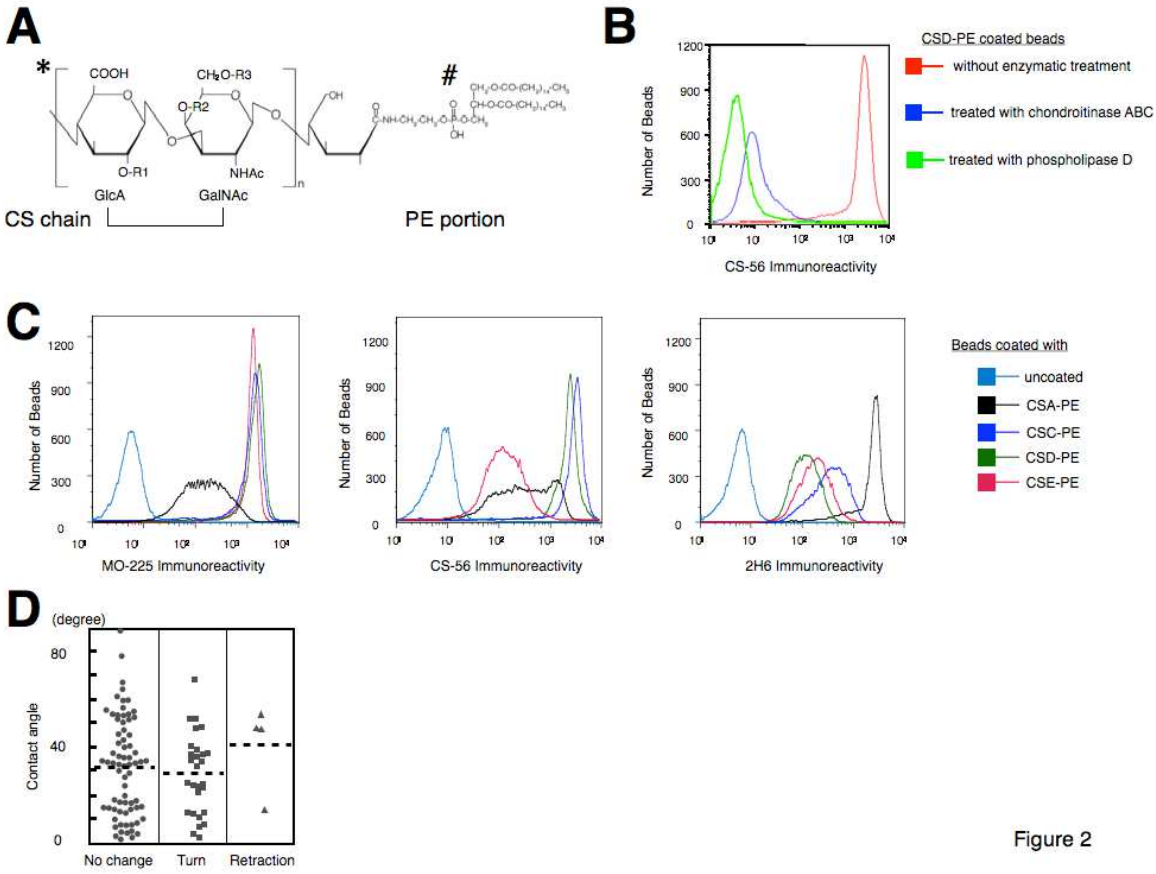
A
COOH
CH2O-R3
O-R2
O-R1
NHAc
GlcA
GalNAc
CS chain
PE portion
B
CSD-PE coated beads
without enzymatic treatment
treated with chondroitinase ABC
treated with phospholipase D
Number of Beads
CS-56 Immunoreactivity
C
Number of Beads
MO-225 Immunoreactivity
CS-56 Immunoreactivity
2H6 Immunoreactivity
Beads coated with
uncoated
CSA-PE
CSC-PE
CSD-PE
CSE-PE
D
(degree)
Contact angle
No change
Turn
Retraction

Figure 2

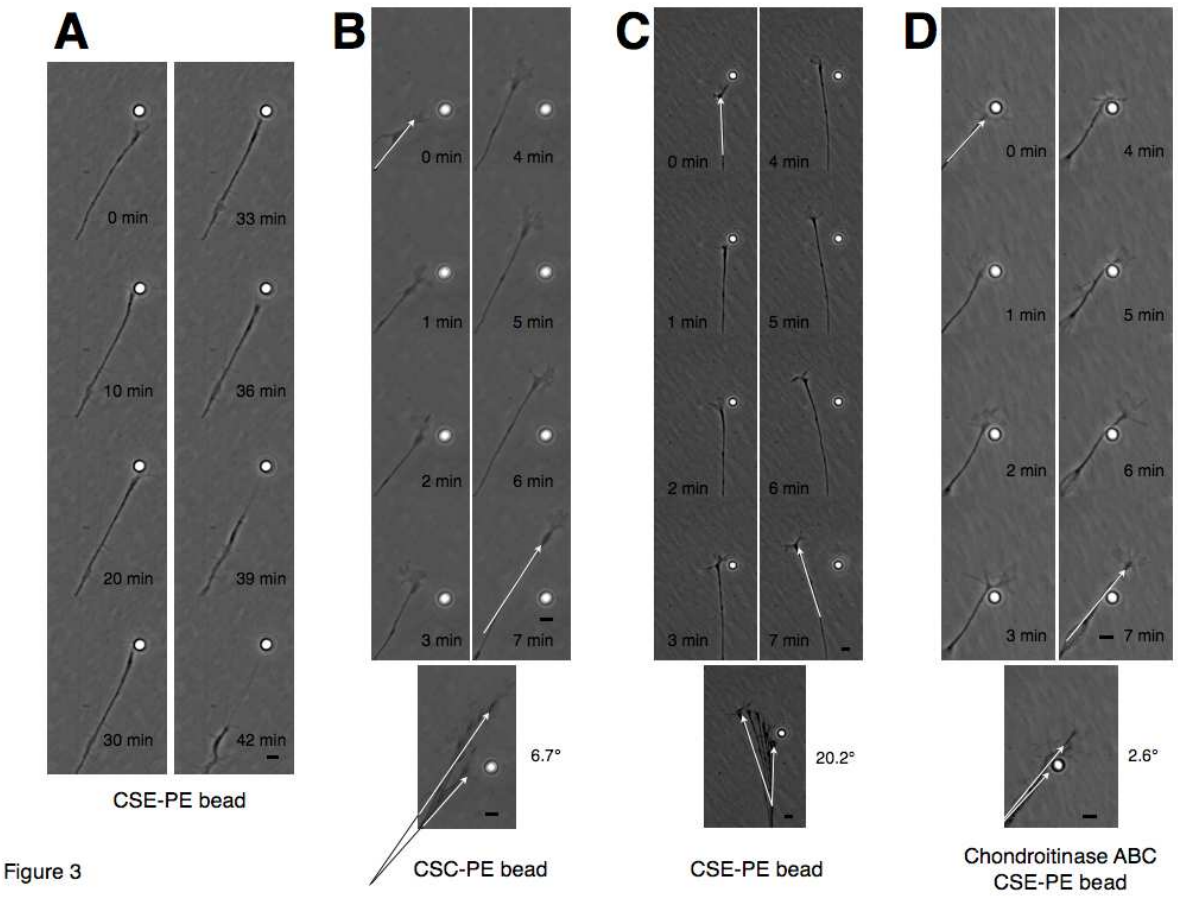
A
0 min
33 min
10 min
36 min
20 min
39 min
30 min
42 min
CSE-PE bead
B
0 min
4 min
1 min
5 min
2 min
6 min
3 min
7 min
6.7°
CSC-PE bead
C
0 min
4 min
1 min
5 min
2 min
6 min
3 min
7 min
20.2°
CSE-PE bead
D
0 min
4 min
1 min
5 min
2 min
6 min
3 min
7 min
2.6°
Chondroitinase ABC
CSE-PE bead

Figure 3

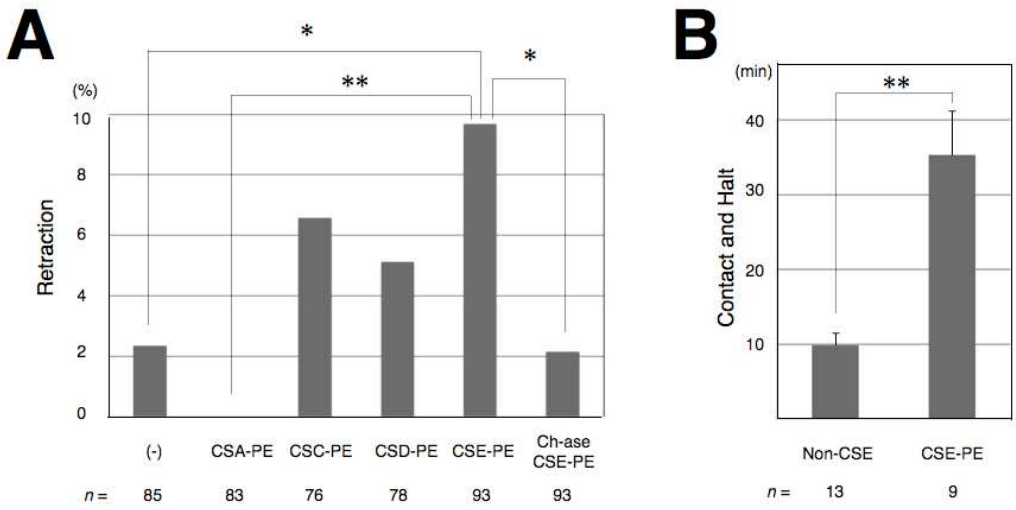
A
*
**
*
(%)
10
8
6
4
2
0
Retraction
(-)
CSA-PE
CSC-PE
CSD-PE
CSE-PE
Ch-ase CSE-PE
n =
85
83
76
78
93
93
B
(min)
40
30
20
10
Contact and Halt
**
Non-CSE
CSE-PE
n =
13
9

Figure 4

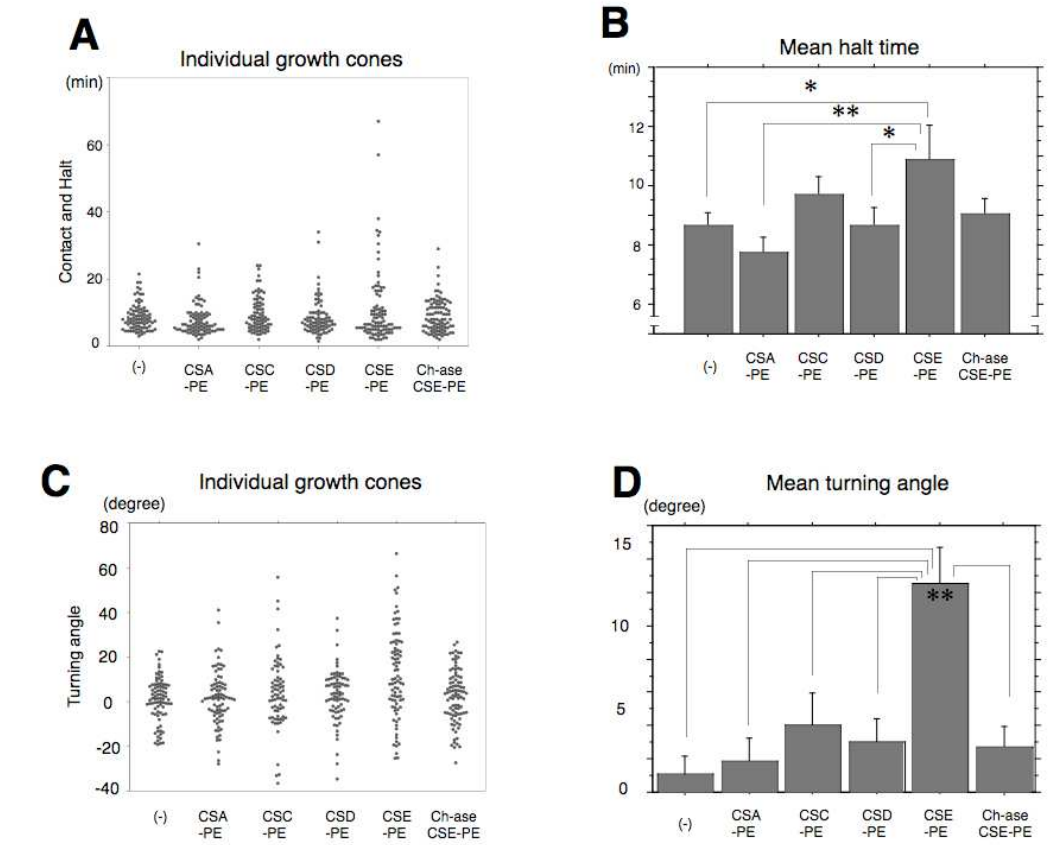
A
Individual growth cones
(min)
Contact and Halt
60
40
20
0
(-)
CSA -PE
CSC -PE
CSD -PE
CSE -PE
Ch-ase CSE-PE
B
Mean halt time
(min)
12
10
8
6
*
**
*
(-)
CSA -PE
CSC -PE
CSD -PE
CSE -PE
Ch-ase CSE-PE
C
Individual growth cones
(degree)
Turning angle
80
60
40
20
0
-20
-40
(-)
CSA -PE
CSC -PE
CSD -PE
CSE -PE
Ch-ase CSE-PE
D
Mean turning angle
(degree)
15
10
5
0
**
(-)
CSA -PE
CSC -PE
CSD -PE
CSE -PE
Ch-ase CSE-PE

Figure 5

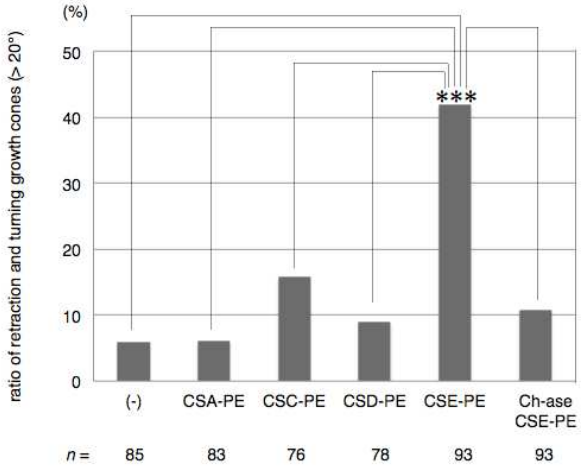
(%)
50
40
30
20
10
0
ratio of retraction and turning growth cones (> 20°)
***
(-)
CSA-PE
CSC-PE
CSD-PE
CSE-PE
Ch-ase CSE-PE
n =
85
83
76
78
93
93

Figure 6